First searches for gravitational waves from r-modes of the Crab pulsar

Binod Rajbhandari, Benjamin J. Owen, Santiago Caride,* and Ra Inta†

Department of Physics and Astronomy, Texas Tech University, Lubbock, Texas, 79409-1051, USA

We present the first searches for gravitational waves from r-modes of the Crab pulsar, coherently and separately integrating data from three stretches of the first two observing runs of Advanced LIGO using the $\mathcal{F}$-statistic. The second run was divided in two by a glitch of the pulsar roughly halfway through. The frequencies and derivatives searched were based on radio measurements of the pulsar's spin-down parameters as described in Caride *et al.,* Phys. Rev. D **100**, 064013 (2019). We did not find any evidence of gravitational waves. Our best 90% confidence upper limits on gravitational wave intrinsic strain were 1.5×10^{-25} for the first run, 1.3×10^{-25} for the first stretch of the second run, and 1.1×10^{-25} for the second stretch of the second run. These are the first upper limits on gravitational waves from r-modes of a known pulsar to beat its spin-down limit, and they do so by more than an order of magnitude in amplitude or two orders of magnitude in luminosity.

I. INTRODUCTION

Rapidly rotating neutron stars might be detectable emitters of long lived quasi-monochromatic radiation known as continuous gravitational waves (GWs) [1]. The emission mechanism for continuous waves could be a nonaxisymmetric mass quadrupole ("mountain") or a current-quadrupolar r-mode. Hence the detection of continuous GWs might help reveal the underlying properties of neutron star interiors. The GW frequencies of many pulsars lie in the most sensitive band of the Laser Interferometer Gravitational-wave Observatory (LIGO), so these rapidly rotating neutron stars are attractive targets for continuous GW searches [2].

The r-modes, whose frequencies are mainly determined by the Coriolis force, are unstable to GW emission [3, 4] even allowing for various damping mechanisms [5]. Hence they might amplify and sustain themselves, and might be the most interesting possibility for continuous GWs. R-modes might play an important role in the spin-downs of the fastest young neutron stars [6] and in the regulation of spin periods of some older accreting neutron stars [7, 8]. Comparison of the GW frequency to the spin frequency determined from timing radio or x-ray pulses could measure the compactness of a pulsar [9], and the existence of r-modes at certain frequencies could constrain the properties of the neutron superfluid [10].

Some GW searches, starting with Ref. [11], have set upper limits on r-mode GW emission. However most of these have been broad band searches for neutron stars not previously known as pulsars. The searches themselves did not take any extra steps to account for r-mode rather than mass-quadrupole emission; rather the results could be interpreted in terms of r-modes [12].

Caride *et al.* [13] showed that dedicated searches for r-modes from known pulsars are feasible. The key is to search the right range of frequencies and frequency derivatives, which are significantly different from the more often considered case of mass-quadrupole emission. Not surprisingly, as with other GW searches for pulsars, the Crab is the first prospect to beat the spin-down limit using LIGO data. The spin-down limit assumes that all the rotational energy is lost in the form of GWs, and represents a milestone a search must beat to have a chance of detection. Recently Fesik and Papa [14] first published an r-mode pulsar search similar to that proposed by Caride *et al.* [13], for another pulsar which is interesting for different reasons; but they did not beat its spin-down limit. The Crab is a relatively nearby pulsar with one of the fastest known spin-down rates, and thus it has one of the highest spin-down limits. Its rotational frequency changes at the rate -3.69×10^{-10} Hz/s [15, 16]. The Crab's pulse timing is constantly measured by electromagnetic (EM) observations, so the spin frequency evolution of the Crab is well known during the LIGO first observing run (O1) and second observing run (O2).

For various reasons we know that the Crab is not emitting GW at or near the spin-down limit. Alford and Schwenzer [17] have argued that, if the r-mode instability operates similarly in all neutron stars, the Crab is probably spinning to slowly to be unstable in the presence of common damping mechanisms. Observations of the Crab nebula indicate that most of the rotational energy is lost powering the nebula via synchrotron and inverse Compton radiation from the pulsar wind, and a few percent is lost in the narrow light beam [18]. Recent GW searches [19, 20] have concluded that less than 0.01% of the Crab's rotational energy loss is through mass-quadrupole gravitational radiation. The braking index n of the Crab (the logarithmic derivative of its spin-down with respect to frequency) is 2.519. This is closer to the $n = 3$ expected for magnetic dipole radiation [21] than to the $n = 7$ expected for r-mode emission [6]. Such a low braking index is another indicator that GW emission is a small fraction of the spin-down limit. How small has not been quantified in a model-independent way or for r-modes. But Palomba [22] found that, for a class of reasonable mass-quadrupole models, the measured braking

---

* Current address: Target Field, 1 Twins Way, Minneapolis,MN, 55403

† Current address: Accelerate, 925B Peachtree Street, NE, PMB 378, Atlanta, GA 30309-3918, USA

Search	Start time (UTC)	End time (UTC)	T_{span} (days)	T_{dat} (days)	SFTs
O1	09/12/15 06:03:57	01/19/16 15:34:47	129.4	133.1	6389
O2 (early)	11/30/16 18:01:57	03/27/17 16:28:25	117.1	128.9	6186
O2 (late)	03/28/17 23:47:38	08/25/17 21:59:34	150.9	167.4	8035

TABLE I. Start and end times of the three searches. The time difference between start and end is T_{span}, while T_{dat} is the live time of the data. The latter can be greater than the former because there are two interferometers.

index of the Crab means it is emitting GW at least a factor of a few below the spin-down limit. We take this to suggest that any r-mode GW signal from the Crab must be at least a factor of a few (in strain) below the spin-down limit. Therefore a GW search must beat the spin-down limit by a factor of a few in amplitude (an order of magnitude in luminosity) to be interesting.

Nevertheless, Caride et $al.$ [13] showed that a search of the Crab with interesting sensitivity is feasible, and we confirm this. We performed searches for the Crab in O1 and O2 data (the publicly available LIGO data sets at the time of writing) using the matched filtering-based technique known as the $\mathcal{F}$-statistic. While we did not find any evidence of a GW signal, we were able to set upper limits beating the spin-down limit by an interesting amount over a wide parameter space.

II. R-MODE SEARCH METHOD

Our search is based on a matched filtering technique known as the $\mathcal{F}$-statistic. Developed by Jaranowski et $al.$ [23] for a single interferometer and by Cutler and Schutz [24] for multiple interferometers, it is a statistical procedure for the detection of the continuous gravitational waves. The $\mathcal{F}$-statistic accounts for the amplitude modulation due to the daily rotation of Earth in a computationally efficient manner. In the presence of a signal, $2\mathcal{F}$ is a non-central chi squared distribution with four degrees of freedom and the non-centrality parameter is approximately the power signal-to-noise ratio. The $\mathcal{F}$-statistic is one half the log of the likelihood function maximized over the unknown strain, phase constant, inclination angle and polarization angle. The main issue when using the $\mathcal{F}$-statistic for this type of search, as described by Caride et $al.$ [13], is to find the ranges of frequencies and frequency derivatives to search.

Pulsars are slowly spinning down due to GW emission and other losses of rotational energy. The evolution of the rotational frequency ν of a spinning down neutron star in the frame of the solar system barycenter is approximated by

$$\nu(t) = \nu(t_0) + \dot{\nu}(t_0)(t - t_0) + \frac{1}{2}\ddot{\nu}(t_0)(t - t_0)^2, \quad (1)$$

where t_0 is a reference time (often the start time of the observation) and dots indicate time derivatives. Generally $\ddot{\nu}$ is not needed for less than a year of integration

time [13]. The frequency evolution is precisely known from electromagnetic observations. It might depart from the above approximation due to timing noise or glitches. Glitches are sudden increases in spin frequency followed by exponential recovery to the pre-glitch frequency [25]. Since the Crab glitched during O2, we divided that search into pre- and post-glitch stretches. More on the Crab pulsar timing for our searches will be discussed in Section III. Timing noise is residual phase wandering of pulses relative to the normal spin down model. Timing noise will deviate GW phases from Taylor series for time scales of a year or longer [26]. Assuming the GW timing noise is similar to the one observed in EM pulses, the mismatch of the Crab ephemeris during LIGO S5 run from the model with no timing noise is less than 1% [27]. So, for all our searches (about four months of data each), timing noise should not significantly mismatch the templates from signal.

For a Newtonian star with spin frequency ν, the r-mode GW frequency is approximately $f = \frac{4}{3}\nu$ [28]. The frequency ratio deviates from 4/3 when corrections due to general relativity, rapid rotation, superfluidity, magnetic fields and core-crust coupling are considered [9]. For fast rotating neutron stars, the elastic restoring force on the crust couples with the Coriolis restoring r-modes resulting in avoided crossings [29]. These are small frequency bands where the simple relation between f and ν is drastically altered as modes change identities. Away from avoided crossings, the r-mode frequency as a function of spin frequency is approximately

$$f = A\nu - B\left(\frac{\nu}{\nu_K}\right)^2 \nu, \quad (2)$$

where ν_K is the Kepler frequency. Here, as in Ref. [13], we neglect effects other than slow rotation and general relativity. The effect of rotation is to decrease the mode frequency in an inertial frame, so A and B are positive.

The ranges of A and B are chosen as in Ref. [13]: We consider a range of compactness of neutron stars ($0.11 \leq M/R \leq 0.31$) [9] which comes from the uncertainty in the equation of state. The range of compactness gives a range $1.39 \leq A \leq 1.57$. The range of B is derived from the relation of f/ν to the ratio of the rotational energy (T) to the gravitational potential energy (W) [30]. For different polytropic indices and compactnesses, the range is 1.23–1.95 times the rotational parameter (T/W). Caride et $al.$ [13] converted T/W into $(\nu/\nu_k)^2$ using $M/R = 0.1$ which

gives a maximum value of $B = 0.195$. The minimum value of B is not well known, so it is taken to be zero.

Our search covers the parameters $(f, \dot{f}, \ddot{f})$. The parameter ranges for our searches are given by Caride *et al.* [13] based on the considerations above:

$$\nu \left[A_{\min} - B_{\max} (\nu/\nu_K)^2 \right] \leq f \leq \nu A_{\max}, \quad (3)$$

$$\dot{\nu} \left[f/\nu - 2B_{\max} (\nu/\nu_K)^2 \right] \leq \dot{f} \leq \dot{\nu} f/\nu, \quad (4)$$

$$0 \leq \ddot{f} \leq \ddot{\nu} f/\nu, \quad (5)$$

where, f is spin frequency, $\dot{f}$ and $\ddot{f}$ are the first and second spin derivative, $A_{min} = 1.39$, $A_{max} = 1.57$, and $B_{max} = 0.195$.

We use the parameter space metric g_{ij} to control the computational cost of our search. The proper distance between two templates is given by the mismatch (μ), which is the loss in signal-to-noise ratio when signal falls exactly between two template waveforms [31]. Templates used to filter the data are chosen with a spacing determined by this mismatch. The template number is given by dividing the proper volume of the parameter space by the proper volume per template [13]:

$$\frac{\sqrt{g}\nu \, |\dot{\nu}| \, \ddot{\nu} B_{\max} (\nu/\nu_K)^2 \left[A_{\max}^2 - A_{\min}^2 \right]}{\left(2\sqrt{\mu/3} \right)^3} \quad (6)$$

where g is the (constant) metric determinant. The parameter space metric is given by [31, 32]

$$g_{ij} = \frac{4\pi^2 T_{\text{span}}^{i+j+2}(i+1)(j+1)}{(i+2)!(j+2)!(i+j+3)}, \quad (7)$$

where i, j stand for parameters $(f, \dot{f}, \ddot{f}) = (0, 1, 2)$ and T_{span} is the time spanned by the observation.

We look at the highest values of the $\mathcal{F}$-statistic $(2\mathcal{F}^*)$ that survived the automated vetoes (described below). The probability that a given value of $2\mathcal{F}^*$ will be observed when no signal is present is given by [11]:

$$P(N; 2\mathcal{F}^*) = NP(\chi_4^2; 2\mathcal{F}^*)[P(\chi_4^2; 2\mathcal{F}^*)]^{N-1} \quad (8)$$

where N is the number of templates (assuming statistically independence) and $P(\chi_4^2; 2\mathcal{F}^*)$ is the central χ^2 cumulative distribution function with four degrees of freedom. The above false alarm probability and corresponding threshold $\mathcal{F}^*$ assume gaussian noise, which is not always the case. A high $2\mathcal{F}$ is not enough to claim the detection, as instrumental lines might act as a periodic signal. We follow each search with the interferometer consistency veto as in (e.g.) Ref. [33], which discards candidates when the joint $2\mathcal{F}$ value from the two interferometers is less than for either single interferometer.

III. THE CRAB PULSAR

The Crab pulsar is the remnant of a supernova explosion seen by Chinese astronomers in the year 1054 AD.

Search	ν (Hz)	$\dot{\nu}$ (Hz/s)	$\ddot{\nu}$ (Hz/s^2)
O1	29.66181	$-3.693830 \times 10^{-10}$	2.41×10^{-20}
O2 (early)	29.64761	$-3.689673 \times 10^{-10}$	1.92×10^{-20}
O2 (late)	29.64380	$-3.688438 \times 10^{-10}$	2.5×10^{-20}

TABLE II. Timing of the Crab pulsar at the beginning of our three different searches. The timing is measured by Jodrell Bank Observatory [16] and interpolated to the start time of each LIGO run. The displayed $\ddot{\nu}$ is the maximum monthly value observed during each run.

This is our first target due to its high spin down limit, which is well above the LIGO O1 sensitivity curve [13]. The rotational energy loss of the pulsar is given by $\dot{E} = 4\pi^2 I_{zz}\nu\dot{\nu} \approx 4.33 \times 10^{31}$ W, where ($I_{zz} = 10^{38}$ kg m^2) is the principal moment of inertia [34]. The spin-down power of the Crab is high enough that, even if r-mode gravitational wave emission is only responsible for a small fraction of it, the GWs could be detectable [13].

The sky location of the Crab pulsar in J2000 coordinates is [16]

$$\begin{aligned} \alpha &= 05^h 34^m 31.94,^s \\ \delta &= +22°00'52.1.'' \end{aligned} \quad (9)$$

The spin frequency and its derivative [16] were obtained from the Jodrell Bank observatory monthly ephemeris and interpolated to the start dates of the LIGO run from the nearest dates of 09/16/2015 (O1), 11/23/2016 (early O2) and 04/16/2017 (late O2). There were no glitches of the Crab during O1, so the whole run was coherently integrated. The Crab glitched at 2017-03-27 22:04:48.000 UTC [25] during the O2 run, approximately halfway through. So we divided the O2 run into two roughly equal stretches. The glitch was very small by Crab standards ($\frac{\Delta\nu}{\nu} = 2.14 \times 10^{-9}$) [25], so we started the search of late O2 a few hours afterwards although the post-glitch relaxation time could be days. Our code does not yet have the ability to combine pre- and post-glitch stretches, so we kept the searches separate and present them as such.

Fast spinning down pulsars are contaminated by timing noise [35], especially when $\ddot{\nu}$ appears negative. During our observational time, the monthly $\ddot{\nu}$ measurement was fluctuating. This might be due to external torque from the magnetosphere and might not affect the high density interior which sources GWs. So we chose the maximum $\ddot{\nu}$ of our search to be the maximum value observed during the observational time and the minimum $\ddot{\nu}$ to be zero. The extra number of templates required by including $\ddot{\nu}$ is factor of a few. Thus the searches were not too expensive due to our probably over-wide range of $\ddot{\nu}$.
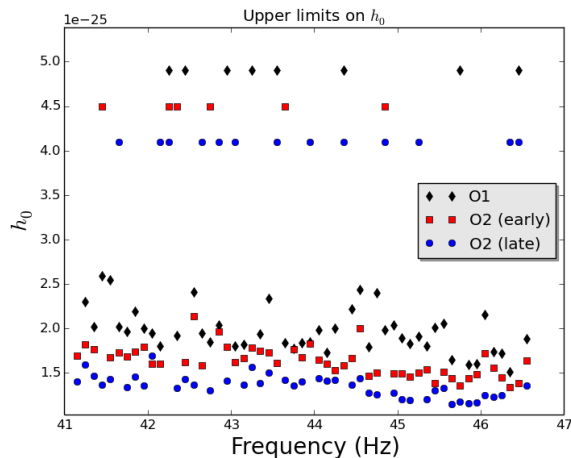
FIG. 1. Upper limits (90% confidence) on intrinsic strain vs. frequency, in 0.1 Hz bands, for our three searches are plotted below the legend. The points arranged in straight lines above the legend indicate "bad" bands (see text).

IV. SEARCH IMPLEMENTATION

We used data from the Gravitational Wave Open Science Center (GWOSC) [36], starting with time-domain strain data sampled at 4 kHz. We downloaded all such O1 data for the official duration of the run (from GPS times 1126051217 to 1137254417) from both interferometers (H1 and L1), gating on only "CBC CAT1" vetoes. These indicate disastrous conditions for the instruments, such as loss of laser power. We ignored the other vetoes used in searches for binary black holes and neutron stars because they are aimed at short-duration disturbances which are not significant for continuous wave searches. We then used the code `lalapps_MakeSFTDAG` from LAL-Suite [37] to generate 1800 s long short Fourier transforms (SFTs), version 2 format, high pass filtered with a knee frequency of 7 Hz and windowed with the default Tukey window. This produced 6,389 SFTs for O1 (3,474 from H1 and 2,915 from L1). A similar procedure for O2 produced 14,231 SFTs (7,242 from H1 and 6,989 from L1). Our r-mode searches used a modified version of a code usually used to search for supernova remnants, most recently in Ref. [33], and was performed on the Texas Tech University High Performance Computing Center's "Quanah" cluster.

The frequency bands of the searches were 41.2–46.6 Hz (O1) and 41.1–46.6 Hz (O2). The minimum and maximum frequencies were rounded down and up respectively from the range in Eq. (3) because we used upper limit bands of a uniform 0.1 Hz. We used a bank of templates with minimal match $\mu = 0.2$. The ideal template numbers for O1, early O2 and late O2 are 2.3×10^9, 9.7×10^8 and 4.0×10^9 respectively. The actual search produced 1.7×10^{10}, 1.2×10^{10} and 3.6×10^{10} templates. The number of templates of each search is around an order of magnitude greater than the ideal number. This is be-

cause the code uses extra templates to cover the boundaries outside the parameter space [11]. The O1, early O2 and late O2 searches used computational times of 1584, 944 and 3892 core hours on Quanah respectively.

Unlike in previous work such as Ref. [33], we did not use the "Fscan veto," based on spectrograms of the data, to eliminate candidates caused by nonstationarity and spectral lines. Applying that veto resulted in the elimination of almost 1/4 of the frequency band of each search. This was due to the wide "wings" of the veto accounting for varying Doppler shifts, spin-down values, and the width of the Dirichlet kernel (used in computing $2\mathcal{F}$). However, the same factors mean that template waveforms have less overlap with stationary instrumental lines than in shorter searches done previously, and so eliminating this veto did not produce an unmanageable number of candidate signals (see below).

After using the interferometer consistency veto, we considered as candidates batch jobs which produced $2\mathcal{F}$ values exceeding a threshold corresponding to a 5% false alarm probability (95% detection confidence) in gaussian noise. We found 29 search jobs with candidates: 16 in O1, 7 in early O2, and 6 in late O2. For each such job we inspected $2\mathcal{F}$ histograms and plots of $2\mathcal{F}$ vs. frequency as in Ref. [38] and later works based on it. All candidate jobs showed distorted histograms and wide band disturbances, indicating instrumental rather than astrophysical origin. Many events just barely passed the interferometer consistency veto, which is a lenient veto. Although we did not use the known spectral lines (and combs) described in Ref. [39] as *a priori* vetoes, we found that many of our candidates were coincident with those lines or with new lines in the combs extending beyond those listed in Ref. [39].

Therefore we do not claim any detection of gravitational waves.

V. UPPER LIMITS

In the absence of a detection, we set upper limits on gravitational wave emission. The method is similar to Ref. Lindblom and Owen [33] among others. Upper limits are the weakest signal that can be detected from our search with a certain probability, in our case chosen to be 90%. This means we set the false dismissal rate to 10%, and the loudest $2\mathcal{F}$ observed (even if vetoed) will set the false alarm rate [38]. Upper limit frequency bands are chosen to be small enough for the interferometer noise to stay reasonably constant. The upper limit band for all the searches is 0.1 Hz.

First, we use a computationally inexpensive Monte Carlo integration to find the intrinsic strain amplitude (h_0) that exceeds the loudest observed $2\mathcal{F}$ 90% of the time. This includes marginalization over inclination and polarization angles, which reduce the actual strain amplitude in the data compared to h_0. Consistent with the $\mathcal{F}$-statistic (and with most other directed searches), we
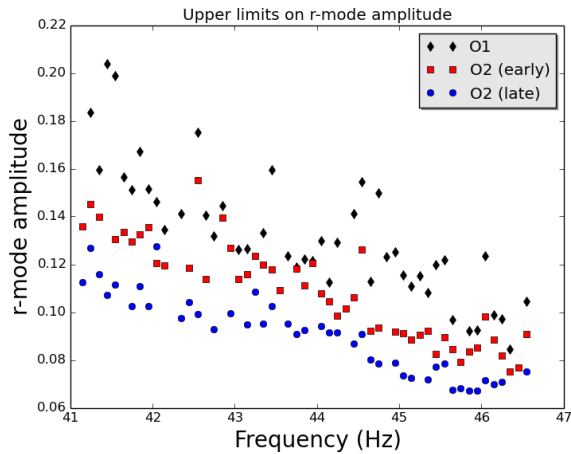
FIG. 2. Upper limits (90% confidence) on r-mode amplitude vs. frequency, in 0.1 Hz bands, for our three searches. "Bad" bands (see text) have been dropped.

used priors corresponding to an isotropic probability distribution of the pulsar's rotation axis. In the case of the Crab the axis is known fairly well [40] and this information could be used to improve the sensitivity of a GW search [41]. However the LALSuite code does not have this capability.

After the Monte Carlo, we use computationally expensive (20–30% of the cost of search) [38] software injection searches to validate the upper limit. In each upper limit band we inject 1000 signals with various h_0. For each h_0 we use variable $f, \dot{f}, \ddot{f}$ and inclination and polarization angles, and consider an injection "detected" if it produces $\mathcal{F} > \mathcal{F}^*$. Comparing this to the Monte Carlo is another check for contaminated frequency bands.

Our upper limits on intrinsic strain in 0.1 Hz bands for our three searches are shown in Fig. 1. In some bands injections indicated that the true false dismissal rate was higher than 10%, typically due to many and/or strong spectral lines. In Fig. 1, for the sake of visibility, these bad bands are given constant values well above the upper limits and thus appear along horizontal lines above the figure legend. The data files are included in the supplemental material to this article [42]. The best 90% confidence level upper limits on intrinsic strain amplitude are 1.5×10^{-25} (O1), 1.3×10^{-25} (early O2) and 1.1×10^{-25} (late O2). O2 upper limits beat the spin-down limit by more than an order of magnitude. Late O2 was the most sensitive because it had the most data and the noise spectrum was better (lower) than the other searches. Upper limits can also be characterized in terms of a statistical factor Θ [32] of the form

$$h_0 = \Theta \sqrt{S_h/T_{\mathrm{dat}}}, \qquad (10)$$

where T_{dat} is the data live time and S_h is the power spectral density of strain noise. We achieved an average $\Theta \simeq 36$, typical for coherent directed searches. Another figure of merit is the "sensitivity depth" [43]

$$\mathcal{D} = \sqrt{S_h}/h_0 = \sqrt{T_{\mathrm{dat}}}/\Theta. \qquad (11)$$

Our searches achieve $\mathcal{D} \simeq 100 \, \mathrm{Hz}^{-1/2}$, comparable to narrow band searches for known pulsars (among the best directed searches).

We can also set upper limits on r-mode amplitude. The coversion of h_0 to r-mode amplitude (α) is shown by Owen [12], who took the fiducial value of moment of inertia ($I_{zz} = 10^{38} \, \mathrm{kg\,m}^2$) and typical $M = 1.4 \, M_\odot$. We convert the upper limit on intrinsic strain h_0 to r-mode amplitude α using

$$\alpha = 0.028 \left(\frac{h_0}{10^{-24}} \right) \left(\frac{r}{1 \, \mathrm{kpc}} \right) \left(\frac{100 \, \mathrm{Hz}}{f} \right)^3. \qquad (12)$$

Upper limits on α are plotted (without the bad bands) in Fig. 2. The best r-mode amplitude upper limits for our different searches are 0.085 (O1), 0.075 (early O2) and 0.067 (late O2).

VI. CONCLUSION

Our searches of LIGO O1 and O2 data for the Crab pulsar did not detect r-mode GWs. However, we set the first upper limits on r-mode GW emission from this pulsar. These upper limits beat the spin-down limit by an order of magnitude in strain or two orders of magnitude in luminosity, and are the first to do so for r-modes from a known pulsar. The corresponding upper limits on r-mode amplitude are not competitive with most predictions of r-mode saturation in young neutron stars such as Ref. [44].

In the near future, with more and better data, we will be able to extend this type of search to longer data sets with lower noise, thereby increasing sensitivity. We will also be able to beat the spin-down limits of more pulsars. With improvements in our code, we will be able to take advantage of the spin axis orientation for those pulsars (such as the Crab) for which it is known and integrate data sets with glitches in them.

ACKNOWLEDGMENTS

[1] K. Glampedakis and L. Gualtieri, Astrophys. Space Sci. Libr. **457**, 673 (2018), arXiv:1709.07049 [astro-ph.HE].

[2] K. Riles, Mod. Phys. Lett. **A32**, 1730035 (2017), arXiv:1712.05897 [gr-qc].

[3] N. Andersson, Astrophys. J. **502**, 708–713 (1998).

[4] J. L. Friedman and S. M. Morsink, Astrophys. J. **502**, 714–720 (1998).

[5] L. Lindblom, B. J. Owen, and S. M. Morsink, Phys. Rev. Lett. **80**, 4843 (1998), gr-qc/9803053.

[6] B. J. Owen, L. Lindblom, C. Cutler, B. F. Schutz, A. Vecchio, and N. Andersson, Phys. Rev. D **58** (1998), 10.1103/physrevd.58.084020.

[7] L. Bildsten, Astrophys. J. Lett. **501**, L89 (1998), arXiv:astro-ph/9804325.

[8] N. Andersson, K. D. Kokkotas, and N. Stergioulas, Astrophys. J. **516**, 307 (1999), arXiv:astro-ph/9806089.

[9] A. Idrisy, B. J. Owen, and D. I. Jones, Phys. Rev. D **91**, 024001 (2015), arXiv:1410.7360 [gr-qc].

[10] E. M. Kantor, M. E. Gusakov, and V. A. Dommes, Phys. Rev. Lett. **125**, 151101 (2020), arXiv:2009.12553 [astro-ph.HE].

[11] J. Abadie, B. P. Abbott, R. Abbott, M. Abernathy, C. Adams, R. Adhikari, P. Ajith, B. Allen, G. Allen, E. Amador Ceron, and et al., Astrophys. J. **722**, 1504–1513 (2010).

[12] B. J. Owen, Phys. Rev. D **82** (2010), 10.1103/physrevd.82.104002.

[13] S. Caride, R. Inta, B. J. Owen, and B. Rajbhandari, Phys. Rev. D **100**, 064013 (2019).

[14] L. Fesik and M. A. Papa, Astrophys. J. **895**, 11 (2020), arXiv:2001.07605 [gr-qc].

[15] "Jodrell Bank Crab Pulsar Monthly Ephemeris," `http://www.jb.man.ac.uk/pulsar/crab.html`.

[16] A. G. Lyne, R. S. Pritchard, and F. Graham Smith, Mon. Not. Roy. Astron. Soc. **265**, 1003 (1993).

[17] M. G. Alford and K. Schwenzer, Astrophys. J. **781**, 26 (2014).

[18] R. Bühler and R. Blandford, Reports on Progress in Physics **77**, 066901 (2014).

[19] B. P. Abbott, R. Abbott, T. D. Abbott, S. Abraham, F. Acernese, K. Ackley, C. Adams, R. X. Adhikari, V. B. Adya, C. Affeldt, and et al., Astrophys. J. **875**, 122 (2019).

[20] R. Abbott et al. (LIGO Scientific, Virgo), Astrophys. J. Lett. **902**, L21 (2020), arXiv:2007.14251 [astro-ph.HE].

[21] A. G. Lyne, C. A. Jordan, F. Graham-Smith, C. M. Espinoza, B. W. Stappers, and P. Weltevrede, Mon. Not. Roy. Astron. Soc. **446**, 857–864 (2014).

[22] C. Palomba, Astron. Astrophys. **354**, 163 (2000), arXiv:astro-ph/9912356.

[23] P. Jaranowski, A. Królak, and B. F. Schutz, Phys. Rev. D **58** (1998), 10.1103/physrevd.58.063001.

[24] C. Cutler and B. F. Schutz, Phys. Rev. D **72**, 063006 (2005).

[25] C. M. Espinoza, A. G. Lyne, B. W. Stappers, and M. Kramer, Mon. Not. Roy. Astron. Soc. **414**, 1679–1704 (2011).

[26] D. I. Jones, Phys. Rev. D **70** (2004), 10.1103/physrevd.70.042002.

[27] G. Ashton, D. I. Jones, and R. Prix, Phys. Rev. D **91**, 062009 (2015).

[28] J. Papaloizou and J. Pringle, Mon. Not. Roy. Astron. Soc. **182**, 423 (1978).

[29] Y. Levin and G. Ushomirsky, Mon. Not. Roy. Astron. Soc. **324**, 917–922 (2001).

[30] S. Yoshida, S. Yoshida, and Y. Eriguchi, Mon. Not. Roy. Astron. Soc. **356**, 217 (2005), arXiv:astro-ph/0406283 [astro-ph].

[31] B. J. Owen, Phys. Rev. D **53**, 6749 (1996), arXiv:gr-qc/9511032 [gr-qc].

[32] K. Wette et al. (LIGO Scientific), *Proceedings, 18th International Conference on General Relativity and Gravitation (GRG18) and 7th Edoardo Amaldi Conference on Gravitational Waves (Amaldi7), Sydney, Australia, July 2007*, Class. Quant. Grav. **25**, 235011 (2008), arXiv:0802.3332 [gr-qc].

[33] L. Lindblom and B. J. Owen, Phys. Rev. D **101** (2020), 10.1103/physrevd.101.083023.

[34] B. Abbott, R. Abbott, R. Adhikari, P. Ajith, B. Allen, and et al., Astrophys. J. **683**, L45 (2008).

[35] A. G. Lyne, Philosophical Transactions of the Royal Society of London. Series A: Physical and Engineering Sciences **341**, 29 (1992).

[36] R. A. et al.(The LIGO Scientific Collaboration and the Virgo Collaboration), "Open data from the first and second observing runs of advanced ligo and advanced virgo," (2019), arXiv:1912.11716 [gr-qc].

[37] T. L. S. Collaboration, "LIGO algorithm library - lalsuite," (2020), https://git.ligo.org/lscsoft/lalsuite.

[38] J. Aasi, B. P. Abbott, R. Abbott, T. Abbott, M. R. Abernathy, F. Acernese, K. Ackley, C. Adams, T. Adams, P. Addesso, and et al., Astrophys. J. **813**, 39 (2015).

[39] P. Covas et al. (LSC), Phys. Rev. D **97**, 082002 (2018), arXiv:1801.07204 [astro-ph.IM].

[40] C.-Y. Ng and R. W. Romani, Astrophys. J. **673**, 411 (2008), arXiv:0710.4168 [astro-ph].

[41] P. Jaranowski and A. Krolak, Class. Quant. Grav. **27**, 194015 (2010), arXiv:1004.0324 [gr-qc].

[42] PRD will insert URL here.

[43] C. Dreissigacker, R. Prix, and K. Wette, Phys. Rev. D **98**, 084058 (2018), arXiv:1808.02459 [gr-qc].

[44] R. Bondarescu, S. A. Teukolsky, and I. Wasserman, Phys. Rev. D **79**, 104003 (2009), arXiv:0809.3448 [astro-ph].